Bioorganic & Medicinal Chemistry 20 (2012) 2498–2505

Contents lists available at SciVerse ScienceDirect

Bioorganic & Medicinal Chemistry

journal homepage: www.elsevier.com/locate/bmc

Synthesis of novel 9-*O*-*N*-aryl/aryl–alkyl amino carbonyl methyl substituted berberine analogs and evaluation of DNA binding aspects

Anirban Basu [a,b], Parasuraman Jaisankar [b], Gopinatha Suresh Kumar [a,b,*]

[a] Biophysical Chemistry Laboratory, CSIR-Indian Institute of Chemical Biology, Kolkata 700 032, India
[b] Chemistry Division, CSIR-Indian Institute of Chemical Biology, Kolkata 700 032, India

ARTICLE INFO

Article history:
Received 2 February 2012
Revised 29 February 2012
Accepted 1 March 2012
Available online 8 March 2012

Keywords:
9-*O*-*N*-Aryl/aryl–alkyl amino carbonyl methyl substituted berberines
Synthesis
DNA binding
Intercalation

ABSTRACT

This manuscript describes the design and synthesis of three 9-O substituted analogs of plant alkaloid berberine to enhance the DNA binding affinity. Three analogs of berberine with aryl/aryl–alkyl amino carbonyl methyl substituent at the 9-position of the isoquinoline chromophore were synthesized and characterized by NMR (^{1}HNMR and ^{13}C NMR) and mass spectroscopy. The products were evaluated for their binding to calf thymus DNA by a wide variety of techniques like spectrophotometry, spectrofluorimetry, circular dichroism, thermal melting, viscosity and isothermal titration calorimetry. The results revealed that these analogs showed more than six times higher binding affinity to DNA compared to berberine. From fluorescence and absorbance studies it was inferred that all the analogs bound to DNA non-cooperatively in contrast to the cooperative binding of the parent alkaloid berberine. The viscosity and ferrocyanide quenching experiments confirmed that the analogs are stronger intercalative binders to DNA useful for potential biological applications. Stronger binding of the analogs was also inferred from circular dichroism studies and thermal melting experiments. Thermodynamics of the binding from isothermal titration calorimetry experiments revealed an entropy driven binding for these analogs compared to the enthalpy driven binding of berberine. The small but negative heat capacity change of the analogs along with the significant enthalpy–entropy compensation phenomenon observed established the involvement of multiple weak noncovalent interactions in the binding process. A comparative study also revealed that the spacer length is also significant in modulating the DNA binding affinities.

1. Introduction

Berberine, the most extensively studied isoquinoline alkaloid, has been characterized to possess multiple pharmacological effects.[1–6] In recent years pharmacological activities of this alkaloid as antihypertensive, antiinflammatory, antioxidant, antidepressant, antidiarrhoeal, cholagogue, hepatoprotective and as antimicrobial agent have been demonstrated.[7–14] The strong antineoplastic effects of berberine appears to suppress the growth of a wide variety of tumor cells.[15,16] Nucleic acid binding properties in terms of duplex and quadruplex structures and topoisomerase inhibition activities were tested for berberine and several derivatives[17–33] and the anticancer activity[1,3] may be interpreted in relation to the strong DNA binding affinity and enzyme inhibition property. An intercalation model of DNA binding has been established for berberine from the recent X-ray data.[34] In several recent articles were also described the selectivity, specificity and thermodynamics of berberine binding to different DNA sequences, triplexes and quadruplex structures.[24–30] In respect of topoisomerase inhibition, the current model suggests that an intercalative as well as a minor groove binding component of berberine may be equally important.[35] Substitutions on the isoquinoline ring have been an important strategy to enhance the efficacy of berberine. Enhanced effect of 9-substituted analogs of berberine on drug-topoisomerase II interactions is well documented from an early investigation based from a comparative study of 9-ethoxycarbonyl berberine, 9-*N*,*N*-dimethylcarbamoyl berberine and 12-bromo berberine (methoxy group at 9-position).[36] The 12-bromo analogue was a stronger DNA binding agent but a much weaker enzyme poison both in vitro and in cell-based assays compared to the others. The results suggested that the proposed drug domain for DNA intercalation is not a major determinant of enzyme inhibition for simple berberine analogs. Rather, the 9-substituent within the domain has a major influence, presumably by facilitating drug interaction with enzyme and/or enzyme-DNA complexes. Various derivatives of berberine including those with substitutions at the 9-position were synthesized or prepared as chemically modified compounds in order to enhance the pharmacological activities[19,21,22] as well as DNA binding affinities.[19,20,31,32]

The binding affinities of berberine with duplex DNA, usually in the range of $1.0–2.0 \times 10^5\ M^{-1}$, are modest and necessitate the

* Corresponding author at: Biophysical Chemistry Laboratory, CSIR-Indian Institute of Chemical Biology, 4, Raja S. C. Mullick Road, Jadavpur, Kolkata 700 032, India. Tel.: +91 33 2472 4049/2499 5723; fax: +91 33 2472 3967.
E-mail addresses: gskumar@iicb.res.in, gsk.iicb@gmail.com (G. Suresh Kumar).

0968-0896/$ - see front matter © 2012 Elsevier Ltd. All rights reserved.
http://dx.doi.org/10.1016/j.bmc.2012.03.006

appropriate structural modification as to serve as a novel DNA-binding agent with enhanced binding affinities. In this paper, we describe the synthesis of three new 9-O-substituted berberine derivatives having *N*-aryl/aryl–alkyl amino carbonyl methyl substituent at the 9-position, their enhanced DNA-binding affinities and the detailed thermodynamic aspects of the interaction. These analogs have been synthesized from the linkage of berberrubine with the intermediates **4a**–**b**, with the aim to assess the effect of the modification at this position on the mode, affinity and energetics of DNA binding. These functional substituents used in the design of DNA-binders, we believe, are expected to increase binding affinities through hydrogen bonding and/or electrostatic interaction with DNA. Thus, the interaction of these berberine derivatives with structural alteration at the 9-position with DNA may provide new insights into the different aspects of association process of berberine with DNA.

2. Results and discussion

2.1. Synthesis of berberine analogs

The synthetic route of 9-O-substituted berberine analogs is shown in Scheme 1. Commercially available berberine chloride (**1**, 1.0 g) when heated at 190 °C under vacuum (10–15 mm) for 45 min underwent selective demethylation to afford berberrubine (**2**) in 65% yield (625 mg).[37] To the solution of either **3a** or **3b** (10 mmol) in dry dichloromethane was added chloroacetyl chloride (11 mmol) dropwise under ice-cold condition. The reaction mixture was stirred at room temperature for 40 min and then it was poured into ice-cold water to decompose the unreacted acid chloride. The resulting solution was neutralized with saturated $NaHCO_3$ solution and the organic layer was extracted with chloroform (3 × 50 ml), dried over Na_2SO_4 and the solvent was removed under reduced pressure. The resulting solid of **4a** or **4b** was utilized to prepare the desired analogs **5a**–**b**. To a solution of berberrubine **2** (1 mmol) in dry CH_3CN (10 ml) was added compounds **4a** or **4b** (1.2 mmol) and the reaction mixture was refluxed for 12 h. The progress of the reaction was monitored by TLC. Then the reaction mixture was cooled to room temperature and the solvent was removed under reduced pressure. The crude product was chromatographed on a neutral Al_2O_3 column and eluted with increasing concentration of MeOH in $CHCl_3$ ($CHCl_3$/MeOH, 99:1–98:2) to afford the desired berberine analogs **5a**–**b**. Similarly, the berberine analogue **6** was prepared from the reaction between berberrubine (**2**) and 2-chloro-*N*-phenyl acetamide (Scheme 1).

2.2. Spectroscopic experiments: Elucidation of the binding affinity parameters

The DNA binding studies of these analogs in comparison with **1** were performed initially using absorption and fluorescence spectroscopy with calf thymus DNA in 10 mM citrate-phosphate buffer of pH 7.0 at 20 °C.[38–42] Hypochromic and bathochromic effects were observed in the visible absorption bands of berberine analogs with three sharp isosbestic points (Fig. 1A) providing unambiguous evidence for the formation of stable complexes with equilibrium between free and bound alkaloid molecules. The bathochromic and hypochromic effects of analogue-DNA complexes were similar to those observed for intercalative ligand–DNA complexation[43] and are suggestive of strong intermolecular interactions involving the overlap of the Π electron cloud of the alkaloid with that of the base pairs. Berberine analogs have a weak intrinsic fluorescence with maximum around 525 nm and a hump around 445 nm when excited at 345 nm that enhanced on binding with deoxyribonucleic acid. Figure 1B shows the results from spectrofluorimetric titration of **6** with DNA. Pronounced enhancement of the fluorescence intensity on binding to CT DNA was observed for the analogs **6**, **5a** and **5b**. Saturation was obtained at P/D (DNA base pair/alkaloid molar ratio) 18, 27 and 34 for **6**, **5a** and **5b** which is much lower than that for **1** where saturation was achieved at a P/D of 38. The binding affinities of the alkaloid analogs were estimated from Scatchard plots fitted to McGhee and von Hippel analysis.[40] The binding of **1** was cooperative as evidenced by the positive slope in the Scatchard plot at low *r* values while the binding of the analogs studied was found to be non-cooperative (negative slope) (Fig. 1C and D). The substitution at the 9-position of BC therefore switched the binding from a cooperative to non-cooperative mode. The intrinsic binding affinity (K_i) values obtained from absorption and fluorescence spectral analysis are presented in Table 1. It can be seen that the K_i values are significantly higher for the analogs compared to **1** and the magnitude varied as **6** > **5a** > **5b** > **1**. The number of excluded sites (*n*) was found to be around 2–3 for each of the analogs. The binding stoichiometry of these molecules to DNA was estimated independently by continuous variation analysis procedure (Job's plot) from fluorescence.[44]

2.3. Binding stoichiometry (Job plot)

For determining the stoichiometry, the alkaloid: DNA molar ratio was varied keeping the total molar concentration constant. The stoichiometry of binding was determined from the molar ratio where maximal binding was observed. The plot of difference

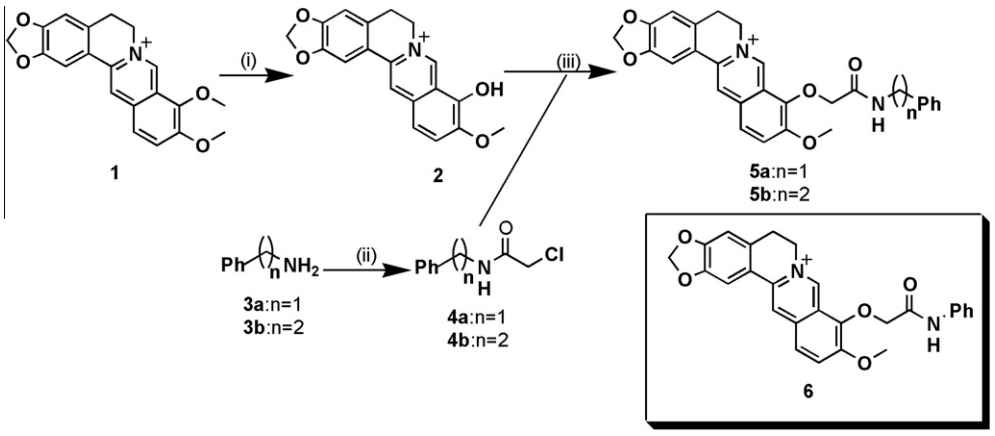

Scheme 1. Reagents and conditions: (i) 190 °C, vacuum (10–15 mm Hg), 45 min; (ii) $ClCH_2COCl$ (1.1 equiv), DCM, rt, 40 min; (iii) CH_3CN, reflux, 12 h.

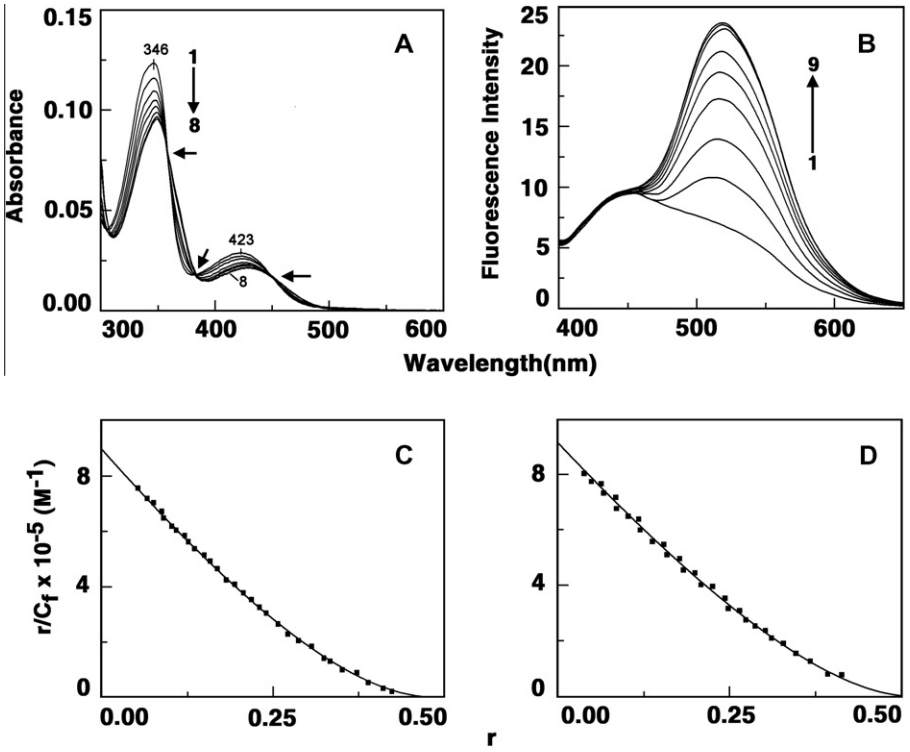

Figure 1. (A) Absorption spectra of **6** (curve 1) with increasing concentration of CT DNA (curves 2–8) in 10 mM CP buffer, pH 7.0. (B) Fluorescence spectra of **6** (curve 1) with increasing concentration of CT DNA (curves 2–9) in 10 mM CP buffer, pH 7.0. (C) Scatchard plot for **6**-CT DNA complexation from absorbance and (D) Scatchard plot for **6**-CT DNA complexation from fluorescence.

Table 1
Association constants and thermodynamic parameters of the binding of berberine and its analogs to CT DNA[a]

Compound	Spectrophotometry	Spectrofluorimetry	Isothermal titration calorimetry				
	$K_i \times 10^{-5}$ (M^{-1})[b]	$K_i \times 10^{-5}$ (M^{-1})	$K_a \times 10^{-5}$ (M^{-1})	n	ΔG^0 (kcal/mol)	ΔH^0 (kcal/mol)	$T\Delta S^0$ (kcal/mol)
1	3.64 ± 0.014	3.64 ± 0.012	1.28 ± 0.05	1.85	−6.84	−3.03	3.81
6	8.93 ± 0.044	9.14 ± 0.041	7.96 ± 0.04	2.00	−7.91	−1.29	6.62
5a	6.85 ± 0.023	6.72 ± 0.025	6.33 ± 0.07	2.44	−7.79	−1.49	6.30
5b	5.92 ± 0.020	5.98 ± 0.017	5.18 ± 0.02	2.86	−7.65	−1.79	5.86

[a] Measured in 10 mM CP buffer, pH 7.0 at 20 °C.
[b] For 1, $K_i = K_{coop} \times \omega$ where K_{coop} is the cooperative of binding affinity and ω is the cooperativity factor. n ($1/N$) is the stoichiometry that may be equated to the number of base pairs spanned by the binding of an alkaloid molecule.

fluorescence intensity (ΔF) at the wavelength maxima versus the mol fraction of the alkaloids revealed a single binding mode in each case. From the inflection point, χ_{ligand} was found to be 0.334, 0.32, 0.29 and 0.26 for **1**, **6**, **5a** and **5b**, respectively. Thus, the number of DNA base pairs bound per berberine analog can be estimated to be around 1.99, 2.12, 2.45 and 2.85, respectively, for **1**, **6**, **5a** and **5b**. The values of stoichiometry are in good agreement with the number of excluded sites obtained from the McGhee-von Hippel analysis of the spectroscopic data.

2.4. Optical melting results

The binding was further tested from optical thermal melting studies.[45] Double stranded calf thymus DNA under the conditions of the experiment had a melting temperature (T_m) value of 65 °C (Fig. 2). The melting temperature of the DNA enhanced in the presence of the analogs and at saturation ΔT_m values of 15.5, 14.0 and 12.0 °C, respectively, were observed for **6**, **5a** and **5b** against a ΔT_m of 9.0 °C for **1** under identical conditions (Fig. 2). Such high stabilization of the DNA helix is essentially due to the strong binding of

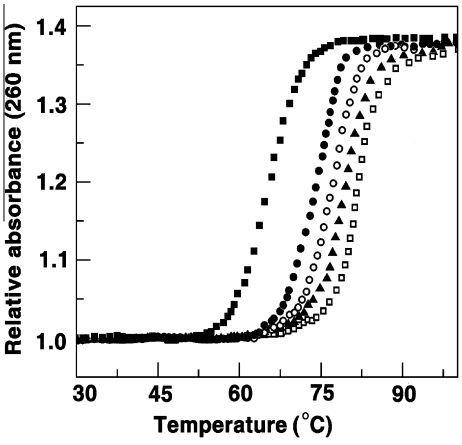

Figure 2. Optical thermal melting profiles of CT DNA (■), CT DNA-**1** (●), CT DNA-**5b** (○), CT DNA-**5a** (▲) and CT DNA-**6** complex (□).

these analogs and reflected better interaction probability of the analogs compared to **1**.

2.5. Intrinsic circular dichroism studies

The association between the berberine analogs and CT DNA was studied by means of circular dichroism spectroscopy.[32] CD spectrum of calf thymus DNA displayed a canonical B-form conformation with a large positive band at 270–280 nm and a negative band at 248 nm. A small positive band at 210 nm was also apparent for the B-form structure. These CD bands of the duplex DNA are caused due to stacking interactions between the base pairs and the helical structure that provide asymmetric environment for the bases. Enhancement of the long wavelength band ellipticity of the DNA was observed in presence of the analogs (Fig. 3). The extent of enhancement was higher for the analogs when compared with the parent alkaloid. This indicates a stronger intercalative binding compared to **1** because of a larger lengthening and consequent weakening of the base stacking interactions. Furthermore, this also suggests closer interaction of the transition moments of the bound analogs with that of the base pairs of DNA. The intercalative mode of binding of these analogs has been independently verified by fluorescence quenching and hydrodynamic methods.

2.6. Fluorescence quenching studies and elucidation of the mode of binding

The intercalative DNA binding mode of berberine has been unequivocally established from the recent X-ray studies.[34] So it may be presumed that, like berberine, these analogs also may intercalate to DNA, but what is the effect of the 9-substituted side chain on the intercalation mode? We probed the DNA binding mode of the analogs in comparison with berberine at first using ferrocyanide quenching experiments.[26,46] This anionic quencher would not be able to penetrate the negatively charged double helix and if these analogs are bound inside the DNA helix strongly by intercalation then little or no change in fluorescence is expected. Stern–Volmer plots for the quenching of the fluorescence of berberine analogs by the DNA clearly indicated that free molecules were quenched efficiently. More quenching was observed in case of **1** and less quenching for the bound analogs **6**, **5a** and **5b** indicating the bound analogs are indeed located in a relatively more protected environment than that of **1**. The quenching constants (K_{sv}) calculated were in the range 200–230 M^{-1} for the unbound alkaloid analogs and 90, 57, 48 and 37 M^{-1}, respectively, for **1**, **6**, **5a** and **5b**. From these results it can be inferred that the bound alkaloid analogs are sequestered away from the solvent confirming strong intercalative binding. The trend in the values suggests that the K_{sv} of **1** is higher than that of **6** and for the others it varied as **1** > **5b** > **5a** > **6**. Thus, this data suggests that **5b** is better intercalated than **1**, and **6** has a much better intercalation capability compared to **5a** and **5b**. These conclusions were also reaffirmed by viscosity studies where length enhancement was maximum with **6**.

2.7. Verification of intercalation by viscosity measurements

The intercalative binding of the analogs was tested by viscosity measurements. Viscometric technique is a well established, and reliable hydrodynamic method[47,48] and the most stringent test for establishing the extension of double stranded DNA helix on intercalation. The original hypothesis of Lerman[49] proposed that the viscosity of a rod like nucleic acid would increase upon complexation on intercalation to accommodate the stacked molecules between the base pairs. This process would result in an increase in the contour length of the DNA. Hence, to further probe the binding mode, the viscosity of the DNA solution was measured in presence of increasing concentrations of the alkaloid analogs and the change in relative viscosities with varying D/P (alkaoid/DNA base pair molar ratio) value were estimated (Fig. 4). The change was found to be more rapidly pronounced for the analogs compared to **1**. Viscosity results are expressed as length enhancement estimated with respect to a standard value (β) of 1.0 for a true intercalator corresponding to a length enhancement of 0.34 nm per bound drug. The β values for **1**, **6**, **5a** and **5b** binding to DNA were found to be 0.70, 0.84, 0.79 and 0.77, respectively. Thus, a much better DNA intercalation scenario may be envisaged for the analogs compared to the parent alkaloid berberine. Therefore, in the confirming viscosity experiment we observed greater length enhancements for **6**, **5a** and **5b** compared to **1** on intercalation to rod like DNA suggesting better intercalation geometry compared to berberine suggesting that the side chain contributes to the stronger binding.

2.8. Energetics of the binding from isothermal titration calorimetry studies

Isothermal titration calorimetry (ITC) was utilized to study the interaction in more details.[43] ITC enables the direct and accurate estimation of the binding affinity and complete thermodynamic parameters of the complexation. Compound **1** and its three analogs

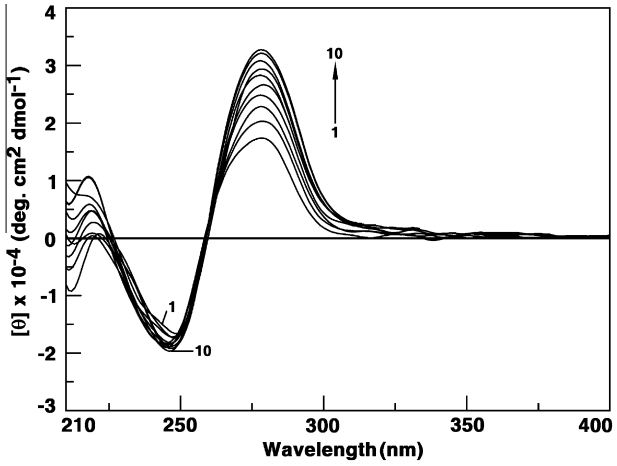

Figure 3. Circular dichroic spectra of CT DNA (curve 1) with increasing concentration of **6** in 10 mM CP buffer, pH 7.0, as represented by curves 2–10.

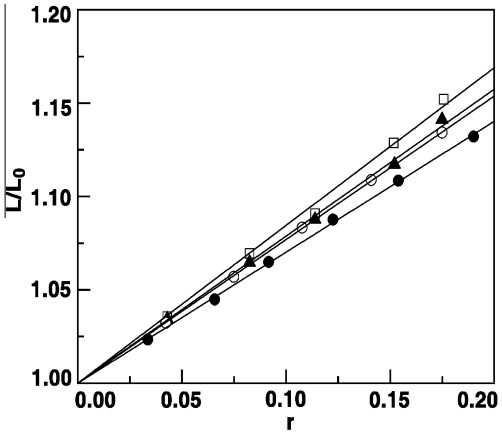

Figure 4. A plot of increase in helix contour length (L/L_o) versus r for the complexation of CT DNA with **6** (□), **5a** (▲), **5b** (○) and **1** (●) in 10 mM CP buffer, pH 7.0, at 20 ± 0.5 °C.

bound to CT DNA exhibiting monophasic binding events that were exothermic, resulting in negative peaks in a plot of power versus time. First of all, exothermic binding was observed in each case and the heat evolved with **1** was higher than that with its analogs. Secondly, the binding of the analogs with double stranded DNA was highly entropy dominated. Since the integrated heat data in the ITC profiles showed only one binding event, they were fitted to a single set of identical sites model. This was also based on the results from single binding mode revealed from the Job plot analysis. A representative ITC thermogram of the titration of **6** with DNA is depicted in Figure 5. The thermodynamic parameters of the interaction elucidated from a single site fitting protocol are presented in Table 1. It can be seen that the binding affinity values for **6**, **5a** and **5b** were $7.96 \times 10^5\ M^{-1}$, $6.33 \times 10^5\ M^{-1}$ and $5.18 \times 10^5\ M^{-1}$, respectively, against the value of $1.28 \times 10^5\ M^{-1}$ for **1**. A comparative bar chart of the K_a values is presented in the Figure 6. The binding affinity values from ITC clearly suggested an increase of affinity from **1** to **6** and a gradual decrease from **5a** to **5b** compared to **6**. The stoichiometry (N) values in the range 0.54–0.35 also decreased going from **1** to **5b**. The binding Gibb's energy (ΔG^0) was −6.84 kcal/mol for **1** that enhanced for all the analogs indicating enhanced binding preference. With the introduction of the side chain the enthalpy change (ΔH^0) was greatly reduced while the entropy change ($T\Delta S^0$) was remarkably increased indicating the entropy domination of the binding for the analogs compared to **1**. The site size (n), which is the reciprocal of stoichiometry (N) values, in the range 1.85–2.86, also enhanced going from **1** to **5b** and are in excellent agreement with the stoichiometry values obtained from Job plot analysis. Comparison of the thermodynamic parameters helps to elucidate the forces that govern the complexation. First of all, with the introduction of the substituent at 9-position a remarkable enhancement in binding affinity was observed. Secondly, the addition of the side chain at the 9-position enhanced the interaction free energy (in absolute values) by an additional 1.07 kcal/mol for **6** compared to **1**, indicating more favorable contacts by the side chain on the DNA. It is also noteworthy that the n values have enhanced because of the involvement of the side chain in the binding process. It is pertinent to observe that the entropic contribution to the binding Gibb's energy enhanced significantly on going from **1** to **6**, indicating clearly the entropy-driven interaction and the strong positive entropy terms is suggestive of the role of the substituent in the disruption and release of water molecules from the grooves on intercalation of **6**, **5a** and **5b** into the DNA helix. The overall binding affinity and the binding site size values obtained from ITC analysis are in excellent agreement with the affinity values and the number of excluded site values from spectroscopy.

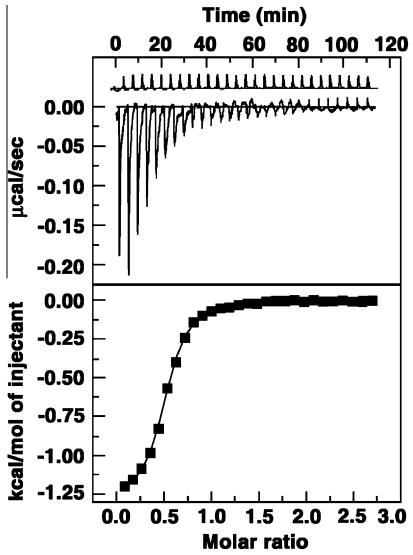

Figure 5. Representative ITC profile for the sequential titration of successive aliquots of **6** to CT DNA in 10 mM CP buffer, pH 7.0 (curve at the bottom), along with the dilution profiles (curves on the top offset for clarity). The top panel represents the raw data and the bottom panel shows the integrated heat data after correction of the heat of dilution. The symbols (■) represent the data points that were fitted to a one-site model and the solid line represents the best-fit data.

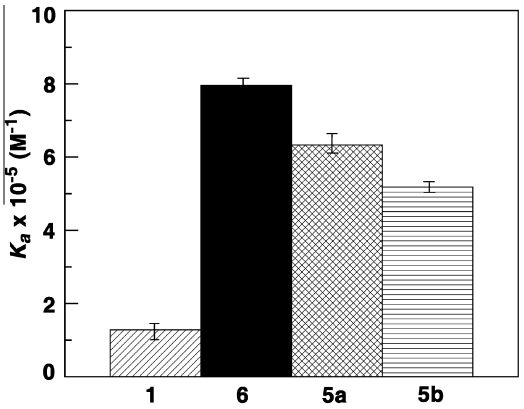

Figure 6. Comparative bar chart depicting the K_a values of **1**, **6**, **5a** and **5b.**

2.9. Temperature dependence of the calorimetric data: Heat capacity changes

The constant pressure heat capacity changes ($\Delta C_p{}^0$) of berberine and its analogs-CT DNA interactions were determined from the temperature dependent enthalpy results employing the standard relationship:

$$\Delta C_p^0 = \delta \Delta H^0 / \delta T \quad (1)$$

Heat capacity change data can provide valuable insights into the type and magnitude of forces involved in the complexation. The thermodynamic parameters were evaluated from ITC studies performed at three temperatures, viz. 10, 20 and 30 °C. As the temperature increased, the association constant (K_a) of the complexation decreased significantly in each case. For the analog **6,** the K_a value decreased from $9.4 \times 10^5\ M^{-1}$ to $6.0 \times 10^5\ M^{-1}$ on increasing the temperature from 10 to 30 °C. Furthermore, there were remarkable changes in the enthalpy and entropy contributions with increasing temperature; while the binding ΔH^0 values increased, the favorable $T\Delta S^0$ values decreased. Nevertheless, only small changes occurred in the Gibb's energy values. The reaction enthalpy and entropy, both of which were strong functions of temperature, compensate each other to make the reaction free energy more or less independent of temperature. Such compensation is observed for many biomolecular interactions[50–52] and suggests the involvement of significant hydrophobic interactions in the binding. The variation of ΔH^0 with temperature (not shown) afforded the $\Delta C_p{}^0$ values. The slopes of the straight lines gave values of −110, −82, −91.5 and −105.5 cal/mol K, respectively, for the binding of **1**, **6**, **5a** and **5b**, respectively. Negative heat capacity values have been observed for a large variety of small molecules binding to DNA and RNA.[43,50,53,54] Furthermore, a negative $\Delta C_p{}^0$ value is usually associated with changes in hydrophobic or polar group hydration and is considered as an indicator of dominant hydrophobic interactions in the binding process. The heat capacity change values are lower for the three analogs compared to the parent alkaloid berberine clearly indicating the influence of the bulky 9-O-substitution on the complexation process. The differences in the $\Delta C_p{}^0$ values may

indicate differences in the release of structured water consequent to the transfer of nonpolar groups into the interior of the helix. First of all, the values of ΔC_p^0 are non-zero and negative indicating temperature dependence of the enthalpy change and significant hydrophobic contribution in the binding process. Secondly, the values of ΔC_p^0 in almost all cases fall within the range 100–500 cal/mol K or are very close to the lower limit that is frequently observed for many ligand–nucleic acid interaction.[53,54] Slightly higher ΔC_p^0 values for **1** compared to the analogs for binding to the DNA may suggest conformational differences in its structure and also differences in the disruption of the water structure around the base pairs of the DNA on complexation. Four types or modes of DNA recognition and binding by small molecules viz. sequence specific, non-specific, minimal sequence specific and structure specific have been discussed by Murphy and Churchill.[55] Small negative ΔC_p^0 values are considered to be the hallmark of a minimal sequence specific binding and hence the slightly negative non-zero ΔC_p^0 value that is observed here for the 9-*O*-berberine analogs-DNA complexation appears to denote structure specific binding. It is known that for DNA intercalators a large hydrophobic contribution to the binding free energy is expected from their aromatic ring system and the binding should be energetically favourable.[53] From the records[56] relationship, $\Delta G_{hyd} = 80(\pm 10) \times \Delta C_p^0$, the free energy contribution from the hydrophobic transfer step of binding of these molecules were calculated. The ΔG_{hyd} values for **1**, **6**, **5a**, **5b** binding to CT DNA were deduced to be −8.80. −6.56, −7.32 and −8.44 kcal/mol, respectively, which are all well within the range that were observed for DNA and RNA intercalating molecules.[50,53,57,58]

3. Conclusion

In summary, we have designed and synthesized three new 9-O-substituted berberine analogs. With respect to DNA binding, these analogs have retained the DNA binding mode, viz. intercalation, but a remarkable amplification of the DNA binding affinity and thermal stabilization of DNA against strand separation was observed. Ferrocyanide quenching and viscosity studies confirmed that all these compounds bound to DNA by intercalation geometry exhibiting stronger intercalative property. The binding affinity of the analogs was dependent on the length of the side chain. The highest binding affinity was for **6** which was six times more than that of **1** under identical conditions. However, further chain elongation gradually reduced the binding affinity. The 9-O-substitution enhanced the thermal stabilization of DNA remarkably. Analog **6** enhanced the stability of the DNA by almost 7 °C higher than that of **1** clearly suggesting strong additional binding effects from the side chain. This indicates that the side chain can effectively participate in H-bonding with either the base pairs or the phosphates of the DNA. The Scatchard binding isotherms showed pronounced cooperative binding for **1** in agreement with the literature data whereas the binding of the analogs was found to be completely non-cooperative. This might suggest significant differences in the mechanism of binding. Circular dichroism studies confirmed that a higher perturbation of the DNA conformation within the B-form was also achieved for the analogs compared with the parent berberine. Thermodynamics of the interaction revealed a larger entropic and a smaller but favorable enthalpic contribution, that increased significantly with temperature, to the binding free energy with the introduction of the *N*-aryl/aryl–alkyl amino carbonyl methyl substituent suggesting the role of release of DNA bound water molecules by the side chain. The small but negative heat capacity change of the analogs along with the significant enthalpy–entropy compensation phenomenon observed confirmed the involvement of multiple weak noncovalent interactions in the binding process. These results may be of potential significance for the design and development of berberine based therapeutic agents with greater efficacy.

4. Materials and methods

4.1. Materials

Calf thymus (CT) DNA was obtained from Sigma–Aldrich Corporation (St. Louis, MO, USA). The concentration of the CT DNA was determined by absorption measurements using the molar extinction coefficient value of 13,200 M^{-1} cm^{-1} at 260 nm expressed in base pairs. Berberine chloride was purchased from Sigma–Aldrich and was used without further purification. The concentrations of **1**, **6**, **5a** and **5b** were determined by applying the molar extinction coefficient (ε) values of 22,500, 25,000, 26,000, 26,500 M^{-1} cm^{-1}, respectively, at the wavelength maximum of 345 nm. All buffer salts and other reagents were of analytical grade or better. Solutions were freshly prepared in the buffer and kept protected in the dark. All experiments were conducted in filtered 10 mM citrate-phosphate (CP) buffer, pH 7.0, prepared in deionised and triple distilled water.

4.2. General procedure for synthesis of berberine analogs

To the solution of *N*-aryl/aryl–alkyl amine (10 mmol) in dry dichloromethane was added chloroacetyl chloride (11 mmol) dropwise under ice-cold condition. Then the reaction mixture was stirred at room temperature for 40 min and then it was poured into ice-cold water to decompose the unreacted acid chloride. The resulting solution was neutralized with saturated $NaHCO_3$ solution and the organic layer was extracted with chloroform (3 × 50 ml), dried over Na_2SO_4 and the solvent was removed under reduced pressure. The resulting solid (1.2 mmol) was added to a solution of berberrubine **2** (1 mmol) in dry CH_3CN (10 ml) and the reaction mixture was refluxed for 12 h. The progress of the reaction was monitored by TLC. Then the reaction mixture was cooled to room temperature and the solvent was removed under reduced pressure. The crude product was chromatographed on a neutral Al_2O_3 column, eluted with increasing concentration of MeOH in $CHCl_3$ ($CHCl_3$/MeOH, 99:1–98:2) to afford the desired berberine analogs.

4.2.1. Synthesis of compound 5a

Berberrubine was treated with compound **4a** according to the general procedure to obtain the desired product as a yellow solid. (24% yield). IR (KBr) ν_{max} 3437, 1686, 1555, 1266 cm^{-1}. UV–Vis (λ_{max}) 228, 265, 344, 421 nm. ^1H NMR (300 MHz, CD_3OD) δ 10.04 (s, 1H), 8.74 (s, 1H), 8.16 (d, *J* = 9.3 Hz, 1H), 8.06 (d, *J* = 9.0 Hz, 1H), 7.69 (s, 1H), 7.60 (d, *J* = 7.8 Hz, 2H), 7.35 (t, *J* = 7.8 Hz, 2H), 7.15 (t, *J* = 7.3 Hz, 1H), 6.99 (s, 1H), 6.13 (s, 2H), 5.13 (s, 2H), 4.96–4.90 (m, 2H), 4.62 (s, 2H), 4.13 (s, 3H), 3.32–3.27 (m, 2H). ^{13}C NMR (150 MHz, CD_3OD) 171.07, 152.42, 151.69, 150.13, 146.97, 143.73, 139.98, 139.94, 135.21, 132.06, 129.76 (1 × 2), 128.82 (1 × 2), 127.71, 125.37, 124.64, 123.43, 121.97, 121.61, 109.56, 106.72, 103.87, 73.09, 57.76, 57.46, 43.96, 28.32. ESIMS *m*/*z*: $[M-Cl]^+$ 469.21. Anal. Calcd. for $C_{28}H_{25}ClN_2O_5$: C, 66.60; H, 4.99; N, 5.55. Found: C, 66.53; H, 5.13; N, 5.73.

4.2.2. Synthesis of compound 5b

Berberrubine was treated with compound **4b** according to the general procedure to obtain the desired product as a yellow solid (57% yield). IR (KBr) ν_{max} 3342, 1652, 1548, 1271 cm^{-1}. UV–Vis (λ_{max}) 228,264,345,423 nm. ^1H NMR (600 MHz, CD_3OD) δ 9.89 (s, 1H), 8.71 (s, 1H), 8.11 (d, *J* = 8.4 Hz, 1H), 8.03 (d, *J* = 9.0 Hz, 1H), 7.66 (s, 1H), 7.27–7.16 (m, 5H), 6.97 (s, 1H), 6.25 (s, 2H), 4.92 (t, *J* = 6.3 Hz, 2H), 4.88 (s, 2H), 4.06 (s, 3H), 3.53 (t, *J* = 7.5 Hz, 2H),

3.27 (t, J = 6.3 Hz, 2H), 2.86 (t, J = 7.2 Hz,2H). ^{13}C NMR (150 MHz, CD_3OD) 171.08, 152.39, 151.65, 150.10, 146.99, 143.66, 140.47, 139.90, 135.21, 132.06, 129.95 (1 × 2), 129.67 (1 × 2), 127.76, 127.58, 125.36, 123.36, 121.95, 121.58, 109.56, 106.72, 103.85, 72.84, 57.81, 57.49, 41.88, 36.65, 28.32. ESIMS m/z: $[M-Cl]^+$ 483.18. Anal. Calcd for $C_{29}H_{27}ClN_2O_5$: C, 67.11; H, 5.24; N, 5.40. Found: C, 67.03; H, 5.35; N, 5.56.

4.2.3. Synthesis of compound 6

Berberrubine was treated with 2-chloro-*N*-phenyl acetamide according to the general procedure to obtain the desired product as a yellow solid (35% yield). IR (KBr) ν_{max} 3267, 1692, 1537, 1262 cm^{-1}. UV–Vis (λ_{max}) 230, 263, 346, 423 nm. ^{1}H NMR (300 MHz, CD_3OD) δ 10.03 (s, 1H), 8.72 (s, 1H), 8.15 (d, J = 9.0 Hz, 1H), 8.05 (d, J = 9.0 Hz, 1H), 7.64 (s, 1H), 7.57 (d, J = 8.4 Hz, 2H), 7.35 (t, J = 7.8 Hz, 2H), 7.15 (t, J = 7.5 Hz, 1H), 6.98 (s,1H), 6.10 (s, 2H), 5.06 (s, 2H), 4.96–4.89 (m, 2H), 4.13 (s, 3H), 3.33–3.32 (m, 2H). ^{13}C NMR (150 MHz, CD_3OD) 169.52, 152.42, 151.61, 150.14, 147.29, 143.99, 139.97, 139.16, 135.30, 132.10, 130.13 (1 × 2), 127.80, 125.93, 125.26, 123.54, 122.02, 121.72 (1 × 2), 121.58, 109.57, 106.75, 103.87, 72.85, 57.90, 57.54, 28.35. ESIMS m/z: $[M-Cl]^+$ 455.30. Anal. Calcd for $C_{27}H_{23}ClN_2O_5$: C, 66.06; H, 4.72; N, 5.71. Found: C, 66.01; H, 4.84; N, 5.86.

4.3. Elucidation of DNA binding by spectroscopic measurements

Measurements were carried out at 20 °C. Binding was monitored spectrophotometrically and fluorimetrically in the alkaloid absorption and emission regions, respectively, after addition of scalar amounts of the CT DNA into freshly prepared alkaloid solutions as described previously.[39,41,42] Spectrophotometric and fluorimetric measurements were made with a Jasco V660 unit (Jasco International Co. Ltd, Hachioji, Japan) and a Shimadzu RF5301 PC fluorimeter (Shimadzu Corporation, Kyoto, Japan), respectively, in thermostated quartz cuvettes of 1 cm path length. Binding data obtained from spectrophotometric and spectrofluorimetric titrations were converted into Scatchard plot of r/C_f versus r as described previously.[25]

The Scatchard isotherms with positive slope at low r values were analyzed using the following McGhee-von Hippel equation for cooperative binding.[40]

$$\frac{r}{C_f} = K_i(1-nr) \times \left(\frac{(2\omega+1)(1-nr)+(r-R)}{2(\omega-1)(1-nr)}\right)^{(n-1)} \left(\frac{1-(n+1)r+R}{2(1-nr)}\right)^2 \quad (2)$$

where, $R = \{[1-(n+1)r]^2 + 4\omega r(1-nr)\}^{\frac{1}{2}}$,

Scatchard plots with negative slopes at low r values were analyzed by the non-cooperative binding model of McGhee and von Hippel as per the following equation:

$$r/C_f = K_i(1-nr)[(1-nr)/\{1-(n-1)r\}]^{(n-1)} \quad (3)$$

Here, K_i is the intrinsic binding constant to an isolated binding site, n is the number of base pairs excluded by the binding of a single alkaloid molecule and ω is the cooperativity factor. All the binding data were analyzed using the Origin 7.0 software (Origin Labs, Northampton, MA, USA) that determines the best-fit parameters to K_i, n and ω to Eq. 2 and K_i and n to Eq. 3.

4.4. Stoichiometry of binding: Job plot

Continuous variation method of Job[44] was employed to determine the binding stoichiometry in each case from fluorescence spectroscopy. Steady state fluorescence measurements were performed in fluorescence free quartz cuvettes of 1 cm path length as described previously.[48,59] All the measurements were performed at constant temperature of 20 ± 1 °C under conditions of continuous stirring. Uncorrected fluorescence spectra were recorded. The fluorescence signal was recorded for solutions where the concentrations of both DNA and the alkaloid were varied while the sum of their concentrations was kept constant. The difference in fluorescence intensity (ΔF) of the alkaloids in the absence and presence of DNA was plotted as a function of the input mol fraction of each alkaloid. Break point in the resulting plot corresponds to the mol fraction of the bound alkaloid in the complex. The stoichiometry was obtained in terms of DNA-alkaloid $[(1-\chi_{alkaloid})/\chi_{alkaloid}]$ where $\chi_{alkaloid}$ denotes the mole fraction of the respective alkaloid. The results reported are averages of at least three experiments.

4.5. Thermal melting studies

Absorbance versus temperature profiles (melting curves) of DNA and alkaloid-DNA complexes were measured on the Shimadzu Pharmaspec 1700 unit equipped with the peltier controlled TMSPC-8 model accessory in eight chambered quartz cuvette of 1cm path length.[45] The temperature was ramped from 20 to 100 °C at a scan rate of 0.5°C/min. monitoring the absorbance changes at 260 nm.

4.6. Circular dichroism studies

The circular dichroism (CD) spectra were recorded on a JASCO J815 spectropolarimeter (Jasco International Co. Ltd, Hachioji, Japan) equipped with a Jasco temperature controller (model PFD 425L/15) interfaced with a HP PC at 20 ± 0.5 °C using instrument parameters reported previously.[32,50] The molar ellipticity values $[\theta]$ (deg. cm^2 dmol^{-1}) were calculated from the equation:

$$[\theta] = [\theta]_{obs}/10lC \quad (4)$$

where $[\theta]_{obs}$ is the observed ellipticity (milli degree), C is the molar concentration and l is the optical path length of the cuvette in cm. The expressed molar ellipticity is in terms of DNA base pairs.

4.7. Fluorescence quenching studies

Quenching studies were carried out with the anionic quencher $[Fe(CN)_6]^{4-}$. Quenching experiments were performed by mixing, in different ratios, two solutions, one containing KCl and the other containing $K_4[Fe(CN)_6]$, in addition to the normal buffer components, at a fixed total ionic strength. Experiments were performed at a constant P/D (DNA base pair/alkaloid molar ratio) monitoring fluorescence intensity as a function of increasing the concentration of the ferrocyanide ions as described in details previously.[26,46] At least four measurements were taken for each set and averaged out. The data were plotted as Stern–Volmer plots of relative fluorescence intensity (F_o/F) versus $[Fe(CN)_6]^{4-}$.

4.8. Hydrodynamic studies

The viscosity of the DNA-alkaloid complexes was determined by measuring the time needed to flow through a Cannon-Manning semi micro size 75 capillary viscometer (Cannon Instruments Company, State College, PA, USA) that was submerged in a thermostated water bath (20 ± 1 °C) as reported previously.[47,48] Small volumes of the alkaloid solution were added to sonicated CT DNA (280 ± 40 base pairs) solution placed in the viscometer. Mixing was effected by slowly bubbling nitrogen gas. Flow times were measured in triplicate to an accuracy of ±0.01 s with an electronic stopwatch Casio Model HS-30W (Casio Computer Co. Ltd, Tokyo, Japan). Relative viscosities for DNA either in the presence or absence of the alkaloids were calculated from the relation:

$$\eta'sp/\eta_{sp} = \{(t_{complex} - t_0)/t_0\}/\{(t_{complex} - t_0)/t_0\} \quad (5)$$

where, η_{sp} and η_{sp} are specific viscosities of the alkaloid-DNA complex and the DNA respectively; $t_{complex}$, $t_{control}$, and t_o are the average flow times for the DNA-alkaloid complex, free DNA and buffer, respectively. The relative increase in length of DNA, $L/L_{o,}$ is obtained from a corresponding increase in relative viscosity using the following equation:

$$L/L_0 = (\eta/\eta_0)^{1/3} = 1 + \beta r \quad (6)$$

where L and L_0 are the contour lengths of DNA in the presence and in the absence of the alkaloid and η and η_0 are the corresponding values of intrinsic viscosity (approximated by the reduced viscosity $\eta = \eta_{sp}/C$ where C is the DNA concentration) and β is the slope of the plot of L/L_0 versus r.

4.9. Isothermal titration calorimetry

Isothermal titration calorimetry (ITC) experiments were carried out on a VP-ITC microcalorimeter (ITC; MicroCal LLC). Instrument control, data acquisition and analysis were performed using the dedicated Origin 7.0 software following methods described previously.[43,54] Briefly, aliquots of degassed alkaloid solutions were titrated from the rotating syringe (stirring speed 290 rpm) into the isothermal sample chamber containing DNA (1.4235 mL) solution. The reference cell was filled with deionized water. The heat liberated or absorbed with each injection of the alkaloid is observed as a peak that corresponds to the power required to keep the sample and reference solutions at identical temperature. The peaks produced over the entire course of the titration were converted to heat output per injection by integration. The area under each heat burst curve was determined by integration using the Origin software. Control experiments were carried out to determine the heat contribution from dilution arising from buffer into DNA and alkaloids into buffer. The resulting corrected injection heats were plotted as a function of the molar ratio. Experimental data were fitted using a non linear least square minimization algorithm to one site binding theoretical curves to provide the binding affinity (K_a), the binding stoichiometry (N), and the enthalpy of binding (ΔH^0). The binding site size has been restricted during the fitting process to values close to that obtained from the spectroscopic data. The binding Gibb's energy (ΔG^0) and the entropic contribution ($T\Delta S^0$) were deduced from standard relationships, $\Delta G^0 = -RT\ln K_a$ ($R = 1.9872$ cal mol^{-1} K^{-1}, $T = 298$ K) and $\Delta G^0 = \Delta H^0 - T\Delta S^0$.

Acknowledgment

This work was supported by grants from the CSIR NWP0036. A. Basu is a NET-Senior Research Fellow of the University Grants Commission, Government of India. The authors thank all the colleagues of the Chemistry and Biophysical Chemistry Laboratories for cooperation and help during the course of this work. The critical comments of the reviewers that enabled us to improve the manuscript are also appreciated.

Supplementary data

Supplementary data associated with this article can be found, in the online version, at doi:10.1016/j.bmc.2012.03.006.

References and notes

1. Choi, M. S.; Oh, J. H.; Kim, S. M.; Jung, H. Y.; Yoo, H. S.; Lee, Y. M.; Moon, D. C.; Han, S. B.; Hong, J. T. *Int. J. Oncol.* **2009**, *34*, 1221.
2. Kulkari, S. K.; Dhir, A. *Eur. J. Pharmacol.* **2008**, *589*, 163.
3. Letasiova, S.; Jantova, S.; Cipak, L.; Muckova, M. *Cancer Lett.* **2006**, *239*, 254.
4. Zhang, R. X.; Dougherty, D. V.; Rosenblum, M. L. *Chin. Med. J.* **1990**, *103*, 658.
5. Birdsall, T. C.; Kelly, G. S. *Altern. Med. Rev.* **1997**, *2*, 94.
6. Imanshahidi, M.; Hosseinzadeh, H. *Phytother. Res.* **2008**, *22*, 999.
7. Liu, J. C.; Chan, P.; Chen, Y. J.; Tomlinson, B.; Hong, S. F.; Cheng, J. T. *Pharmacology* **1999**, *59*, 283.
8. Cheuh, W. H.; Lin, J. Y. *Food Chem.* **2012**, *131*, 1263.
9. Shirwaikar, A.; Shirwaikar, A.; Rajendran, K.; Punitha, I. S. R. *Biol. Pharm. Bull.* **2006**, *29*, 1906.
10. Peng, W. H.; Lo, K. L.; Lee, Y. H.; Hung, T. H.; Lin, Y. C. *Life Sci.* **2007**, *81*, 933.
11. Baird, A. W.; Taylor, C. T.; Brayden, D. J. *Adv. Drug Delivery Rev.* **1997**, *23*, 111.
12. Szmaz, Z.; Desperak-Naciazek, A.; Obojska, K. *Dissertations Pharm.* **1965**, *17*, 429.
13. Janbaz, K. H.; Gilani, A. H. *Fitoterapia* **2000**, *71*, 25.
14. Yan, D.; Jin, C.; Xiao, X. H.; Dong, X. P. J. *Biochem. Biophys. Methods* **2008**, *70*, 845.
15. Sun, Y.; Xun, K.; Wang, Y.; Chen, X. *Anticancer Drugs* **2009**, *20*, 757.
16. Tang, J.; Feng, Y.; Tsao, S.; Wang, N.; Curtain, R.; Wang, Y. *J. Ethnopharmacol.* **2009**, *126*, 5.
17. Maiti, M.; Suresh Kumar, G. . *Med. Res. Rev.* **2007**, *27*, 649.
18. Maiti, M.; Suresh Kumar, G. *Top. Heterocycl. Chem.* **2007**, *10*, 155.
19. Pang, J. Y.; Qin, Y.; Chen, W. H.; Luo, G. A.; Jiang, Z. H. *Bioorg. Med. Chem.* **2005**, *13*, 5835.
20. Chen, W. H.; Pang, J. Y.; Qin, Y.; Peng, Q.; Cai, Z.; Jiang, Z. H. *Bioorg. Med. Chem. Lett.* **2005**, *15*, 2689.
21. Pang, J. Y.; Long, Y. H.; Chen, W. H.; Jiang, Z. H. *Bioorg. Med. Chem.* **2007**, *17*, 1018.
22. Ma, Y.; Ou, T. M.; Hou, J. Q.; Lu, I. J.; Tan, J. H.; Gu, L. Q.; Huang, Z. S. *Bioorg. Med. Chem.* **2008**, *16*, 7582.
23. Li, T. K.; Bathory, E.; La Voie, E. J.; Srinivasn, A. R.; Olson, W. K.; Sauer, R. R. *Biochemistry* **2000**, *39*, 7107.
24. Grycova, L.; Dostal, J.; Marek, R. *Phytochemistry* **2007**, *68*, 150.
25. Bhadra, K.; Maiti, M.; Suresh Kumar, G. *DNA Cell Biol.* **2008**, *27*, 675.
26. Sinha, R.; Suresh Kumar, G. *J. Phys. Chem. B* **2009**, *113*, 13410.
27. Bhadra, K.; Maiti, M.; Suresh Kumar, G. *Biochim. Biophys. Acta* **2008**, *1780*, 1054.
28. Arora, A.; Balasubramanian, C.; Kumar, N.; Agarwal, S.; Ojha, R. P.; Maiti, S. *FEBS J.* **2008**, *275*, 3971.
29. Bhadra, K.; Suresh Kumar, G. *Biochim. Biophys. Acta* **2011**, *1810*, 485.
30. Franceschin, M.; Rossetti, L.; D'Ambrosio, A.; Schirripa, S.; Bianco, A.; Ortaggi, G.; Savino, M.; Schultes, C.; Neidle, S. *Bioorg. Med. Chem.Lett.* **2006**, *16*, 1707.
31. Bhowmik, D.; Hossain, M.; Buzzetti, F.; D'Auria, R.; Lombardi, P.; Suresh Kumar, G. *J. Phys. Chem. B* **2012**, *116*, 2314.
32. Islam, M. M.; Basu, A.; Hossain, M.; Sureshkumar, G.; Hotha, S.; Suresh Kumar, G. *DNA Cell Biol.* **2011**, *30*, 123.
33. Li, X. L.; Hu, Y. J.; Wang, H.; Yu, B. Q.; Yue, H. L. *Biomacromolecules* **2012**, *13*, 873.
34. Ferraroni, M.; Bazzicalupi, C.; Bilia, A. R.; Gratteri, P. *Chem. Commun.* **2011**, *47*, 4917.
35. Pilch, D. S.; Yu, C.; Makhey, D.; La Voie, E. J.; Srinivasan, A. R.; Olson, W. K.; Sauers, R. R.; Breslauer, K. J.; Geacintov, N. E.; Liu, L. F. *Biochemistry* **1997**, *36*, 12542.
36. Krishnan, P.; Bastow, K. F. *Anti-Cancer Drug Des.* **2000**, *15*, 255.
37. Iwasa, K.; Kim, H. S.; Wataya, Y.; Lee, D. U. *Eur. J. Med. Chem.* **1998**, *33*, 65.
38. Chaires, J. B.; Dattagupta, N.; Crothers, D. M. *Biochemistry* **1982**, *21*, 3933.
39. Bhadra, K.; Maiti, M.; Suresh Kumar, G. *Biochim. Biophys. Acta* **2007**, *1770*, 1071.
40. McGhee, J. D.; von Hippel, P. H. *J. Mol. Biol.* **1974**, *86*, 469.
41. Bhadra, K.; Maiti, M.; Suresh Kumar, G. *Chem. Biodivers.* **2009**, *6*, 1323.
42. Bhadra, K.; Maiti, M.; Suresh Kumar, G. *Biochim. Biophys. Acta* **2008**, *1780*, 298.
43. Hossain, M.; Suresh Kumar, G. *J. Chem. Thermodyn.* **2009**, *41*, 764.
44. (a) Job, P. *Ann. Chim.* **1928**, *9*, 113; (b) Huang, C. Y. *Methods Enzymol.* **1982**, *27*, 509.
45. Hossain, M.; Suresh Kumar, G. *Mol. Biosyst.* **2009**, *5*, 1311.
46. Giri, P.; Suresh Kumar, G. *Mol. Biosyst.* **2008**, *4*, 341.
47. Maiti, M.; Nandi, R.; Chaudhuri, K. *FEBS Lett.* **1982**, *142*, 280.
48. Sinha, R.; Islam, M. M.; Bhadra, K.; Suresh Kumar, G.; Banerjee, A.; Maiti, M. *Bioorg. Med. Chem.* **2006**, *14*, 800.
49. Lerman, L. S. *J. Mol. Biol.* **1961**, *3*, 18.
50. Islam, M. M.; Roy Chowdhury, S.; Suresh Kumar, G. *J. Phys. Chem. B* **2009**, *113*, 1210.
51. Chaires, J. B. *Arch. Biochem. Biophys.* **2006**, *453*, 26.
52. Jen-Jacobson, L.; Engler, L. E.; Jacobson, L. A. *Structure* **2000**, *8*, 1015.
53. Guthrie, K. M.; Parenty, A. D. C.; Smith, L. V.; Cronin, L.; Cooper, A. *Biophys. Chem.* **2007**, *126*, 117.
54. Ren, J.; Jenkins, T. C.; Chaires, J. B. *Biochemistry* **2000**, *39*, 8439.
55. Murphy, F. V.; Churchill, M. E. *Structure* **2000**, *15*, R83.
56. Record, M. T., Jr.; Anderson, C. F.; Lohman, T. M. Q. *Rev. Biophys.* **1978**, *11*, 103.
57. Hossain, M.; Suresh Kumar, G. *J. Chem. Thermodyn.* **2010**, *42*, 1273.
58. Roy Chowdhury, S.; Islam, M. M.; Suresh Kumar, G. *Mol. Biosyst.* **2010**, *6*, 1265.
59. Giri, P.; Suresh Kumar, G. *Arch. Biochem. Biophys.* **2008**, *474*, 183.